American Journal of Engineering Research (AJER)
e-ISSN: 2320-0847 p-ISSN: 2320-0936
Volume-15, Issue-6, pp-114-127
www.ajer.org
Research Paper Open Access

Conceptual Design to Mitigate Corrosion in Natural Gas Transportation Systems

DICKSON NGOWARI DICK and EMEKA OKAFOR
Department of Petroleum and Gas Engineering, University of Port Harcourt, Nigeria.

Abstract
Internal corrosion remains a major integrity threat to wet natural gas pipelines, especially in CO_2-rich environments. This study presents a simulation-driven conceptual design for corrosion mitigation using Aspen HYSYS multiphase flow modelling. Four wet gas streams from a field in Niger Delta with CO_2 content of 2.2-2.9 mol% were simulated in a 10-inch carbon steel pipeline. The Beggs and Brill correlation was used for hydraulic analysis, while the de Waard model was applied for CO_2 corrosion prediction under varying pH (4.0-7.0). Results showed that CO_2 corrosion is the dominant mechanism, with rates ranging from 0.66 in/yr at pH 7.0 to 1.65 in/yr at pH 4.0. Corrosion was highest at the pipeline inlet due to high turbulence. Fluid velocities (66-72 ft/s) exceeded the API RP 14E erosional velocity limit (≈20 ft/s) by a factor of over 3, indicating severe erosion-corrosion risk. An Integrated pH-Velocity-Corrosion Management Strategy (PVCMS) is proposed, incorporating upstream pH stabilization (6.0-6.5), velocity control, high-shear corrosion inhibitors, internal coatings, and real-time monitoring. The framework is expected to reduce corrosion rates below 0.05 in/yr, significantly extending pipeline service life. This study demonstrates the value of integrating process simulation with corrosion modelling for proactive pipeline integrity management in wet gas systems.
Keywords: *CO_2 corrosion, wet gas pipeline, Aspen HYSYS, erosion-corrosion, pH control, pipeline integrity, conceptual design, Niger Delta*

Date of Submission: 14-06-2026 Date of acceptance: 27-06-2026

I. Introduction

Natural gas is a critical component of the global energy mix due to its relatively low carbon emissions, high thermal efficiency, and versatility across industrial, commercial, and domestic sectors (Gurbanov, 2021) and plays a vital role as a transitional fuel in the global energy transition. The economic implications of corrosion are substantial. Corrosion-related failures account for significant maintenance costs, repair expenditures, operational downtime, and infrastructure replacement expenses (Joseph, et al, 2022; Koch, et al, 2016). Beyond economic losses, corrosion-induced failures pose severe safety hazards, including gas leaks, fire outbreaks, and explosions (Bu, et al, 2025; Rusin, and Stolecka, 2021).

Environmental consequences are equally critical, natural gas leaks resulting from corrosion contribute to greenhouse gas emissions and environmental degradation (Lu et al, 2025; Lu et al, 2023). These risks underscore the necessity for comprehensive corrosion management frameworks. However, internal corrosion in wet gas pipelines, primarily driven by CO_2 (sweet corrosion), poses significant safety, economic, and environmental risks (Askari et al., 2019).. Traditional mitigation approaches are often reactive. This study adopts a predictive, simulation-driven approach to develop a conceptual corrosion mitigation design for wet gas pipelines in the Niger Delta.

II. Methodology

The study employed a quantitative simulation-based research design and numerical modelling and engineering simulation tools were used to predict corrosion behaviour under varying operating conditions

Gas Stream Composition Analysis
Four wet gas streams were obtained from a field in Niger Delta and their compositional data are presented in Table 1.

Table 1: Composition of Wet Gas Streams (%)

Component	Gas Stream 1	Gas Stream 2	Gas Stream 3	Gas Stream 4
N_2	0.037	0.086	0.152	0.830
CO_2	2.876	2.941	2.198	2.833
CH_4	81.576	80.220	83.776	79.545
C_2H_6	5.337	6.095	5.365	5.791
C_3H_8	2.769	3.459	3.003	3.681
i-C_4	0.625	0.620	0.581	0.719
n-C_4	1.015	1.115	0.945	1.112
i-C_5	0.456	0.445	0.413	0.500
n-C_5	0.370	0.353	0.312	0.378
C_6	0.996	0.878	0.717	0.912
C_7	0.918	0.775	0.629	0.810
C_8	0.920	0.826	0.602	0.882
C_9	0.608	0.511	0.364	0.525
C_{10}	0.343	0.360	0.219	0.321
C_{11}+	1.154	1.314	0.724	1.161

Reservoir Conditions

The operating pressure, temperature, depth, and acidity of each stream are shown in Table 2.

Table 2: Reservoir Operating Conditions

Parameter	GS1	GS2	GS3	GS4
Pressure (bar)	318.2	323.6	297.8	318.2
Temperature (°C)	92	94	87.1	92
Reservoir	A	C	Xvb	A
Depth (m)	3190.2	3274.9	3018	3226.5
pH	7.0	6.0	5.0	4.0

The pH values were varied deliberately to study the influence of fluid acidity on corrosion severity.

Pipeline System Description

The wet gas was assumed to be transported through a buried carbon steel pipeline. Underground installation was selected for safety, environmental protection, and vandalism prevention.

Tale 3. Pipeline Specifications

Parameter	Value
Pipe Material	Mild Steel
Pipe Schedule	Schedule 40
Nominal Size	10 inch
Internal Diameter	10.02 inch
Outside Diameter	10.75 inch
Roughness	1.5×10^{-4} inch
Thermal Conductivity	45 W/m·K

Table 4. Ground Properties

Parameter	Value
Soil Type	Dry Peat
Ground Conductivity	0.17 W/m·K
Burial Depth	2.5 ft

Pipeline Profile Modeling

The pipeline route consists of inclined and horizontal sections. Elevation changes influence liquid accumulation, pressure drop, slugging tendency, and localized corrosion. Ten pipeline segments were modelled using coordinate data shown in Table 5.

Table 5: Pipeline Coordinates

Segment	Length (ft)	Elevation (ft)
1	0	0.00
2	79	3.28
3	223	-3.28
4	335	-1.64
5	476	1.31
6	591	3.28
7	814	3.28
8	951	2.62
9	1312	0.00
10	1575	0.00
11	1870	0.00

Each coordinate junction was assumed to be a welded joint**,** due to the need for high mechanical integrity under high-pressure gas service.

Process Simulation Procedure

All fluid compositions, pipeline dimensions, thermal properties, and profile coordinates were entered into a steady-state multiphase flow simulation environment such *Aspen HYSYS,*. The same pipeline geometry was used for all four gas streams to ensure consistency.

Flow Correlation Used

Because the pipeline includes horizontal and inclined sections, the Beggs and Brill correlation was selected for pressure drop and holdup prediction. This model is widely accepted for multiphase flow in pipelines with varying inclinations.

CO_2 Corrosion Modeling

CO_2 dissolves in condensed water to form carbonic acid:

$$CO_2 + H_2O \rightarrow H_2CO_3 \quad .1$$

Carbonic acid attacks mild steel, causing generalized and localized corrosion.

The corrosion rate was predicted using the de Waard Model**,** which is one of the most widely used empirical models for sweet corrosion prediction in oil and gas pipelines.

The de Waard model relates corrosion rate to:

1. CO_2 partial pressure
2. Temperature
3. pH
4. Flow velocity
5. Protective iron carbonate film formation

A generalized form is:

$$CR = f(P_{CO_2}, T, pH, V) \quad 2$$

Where:

CR = corrosion rate (mm/y)

P_{CO_2} = partial pressure of CO_2

T = temperature

V = velocity

Simulation Cases

Four acidity levels were simulated:

pH = 7.0 , pH = 6.0 , pH = 5.0 and pH = 4.0

This enabled evaluation of corrosion severity from neutral to strongly acidic conditions.

Erosion Analysis

Corrosion can be accelerated when high-velocity fluids remove protective films from the pipe wall. This mechanism is called erosion-corrosion**.**The erosional velocity was evaluated using API RP 14E equation:

$$V_e = \frac{C}{\sqrt{\rho_m}} \qquad 3$$

Where:

V_e= erosional velocity (ft/s) , C = empirical constant , ρ_m = mixture density , Values of constant C: , 100 for continuous flow and 125 for intermittent flow

If actual gas velocity exceeds erosional velocity, pipe wall damage risk increases.

Slug Flow Analysis

Slugging causes intermittent liquid accumulation and high wall shear stress, which can intensify localized corrosion. To predict flow regime and slug characteristics, the following models were applied:

Translational Velocity Model

The Bendiksen model was used for slug translational velocity prediction.

Liquid Holdup Model

The Gregory et al. model was used for estimation of liquid holdup in the slug body.

Friction Factor Model

The Colebrook–White equation was used for turbulent flow friction factor prediction

$$\frac{1}{\sqrt{f}} = -2\log\left(\frac{e}{3.7D} + \frac{2.51}{Re\sqrt{f}}\right) \qquad 4$$

Data Analysis Technique

Simulation outputs analysed included:

i. Pressure profile
ii. Temperature profile
iii. Gas velocity
iv. Liquid holdup
v. Flow regime
vi. CO_2 partial pressure
vii. Predicted corrosion rate
viii. Erosion risk index

Results were compared across the four gas streams using tables, graphs, and trend analysis.

Validation of Methodology

The selected models are widely accepted in petroleum engineering practice:

1. Beggs and Brill for multiphase pipeline hydraulics
2. de Waard for sweet corrosion prediction
3. API RP 14E for erosion screening
4. Colebrook-White for friction losses

This ensures technical reliability of predictions.

III. RESULTS AND DISCUSSION

Gradient Profiles

Three major gradients were generated from the simulation:

1. Static gradient
2. Friction gradient
3. Acceleration gradient

The figures 1 and 2 below are graphical representation of these gradients as it affects corrosion of the pipe material.

The friction gradient profile in figure 1, shows that internal corrosion risk varies along the pipeline due to changing hydraulic conditions. High friction gradient zones indicate high velocity, turbulence, and wall shear stress, which can remove protective films and accelerate corrosion. Low friction gradient zones may encourage water accumulation, solid deposits, and stagnant conditions that promote pitting and under-deposit corrosion. The gradual increase in friction gradient downstream may also suggest increasing pipe wall roughness caused by ongoing corrosion or scale buildup. Overall, sections with abnormal friction gradient behavior should be prioritized for corrosion monitoring, inhibitor treatment, pigging, and thickness inspection (Nesic, 2007; Revie and Uhlig, 2011) and the overall corrosion risk zones is shown in table 6

Table 6: Overall Corrosion Risk Zones

Pipeline Section	Flow Behavior	Corrosion Risk
0–700 ft	High turbulence/fluctuation	Very High
800–3400 ft	Stable moderate flow	Medium
3400–3800 ft	Low friction/stagnation tendency	High (localized)
3800–8300 ft	Increasing resistance/roughness	High

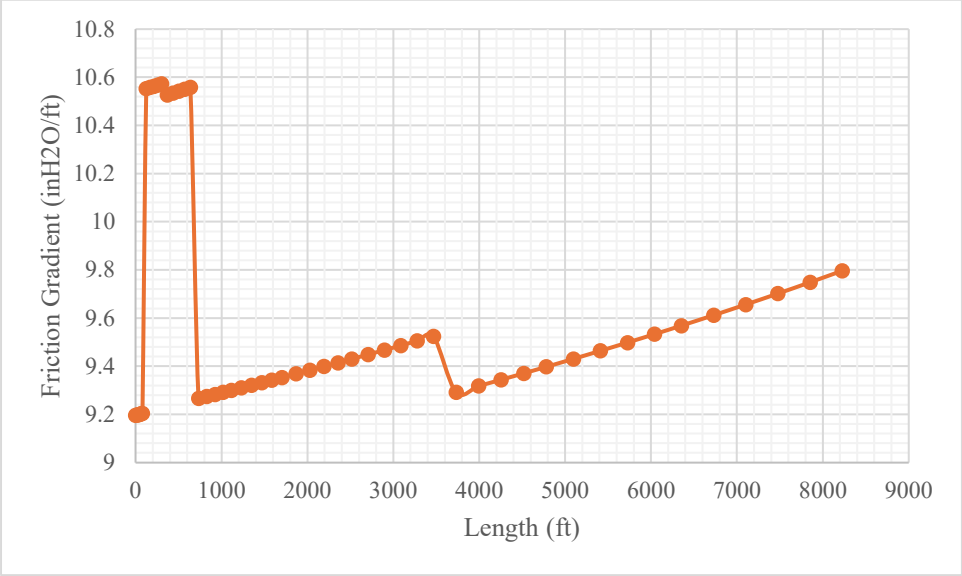

Figure 1 Friction Gradient

The pressure gradient profile in figure 2 suggests that corrosion risk is greatest near the pipeline inlet, where sharp changes in static gradient can cause multiphase flow instability, liquid hold-up, and breakdown of protective films, thereby accelerating internal corrosion. In downstream sections, although flow conditions are more stable, localized corrosion may still occur due to low-velocity liquid accumulation and water settling (Nesic, 2007; Revie & Uhlig, 2008) and the overall corrosion risk zone is shown in table 7

Table 7: Overall Corrosion Risk Zones

Pipeline Section	Flow Behaviour	Corrosion Risk
0–800 ft	Highly unstable gradient	**Very High**
800–3500 ft	Stable moderate flow	**Moderate**
3500–8200 ft	Low gradient / possible stagnant zones	**Moderate to High (localized)**

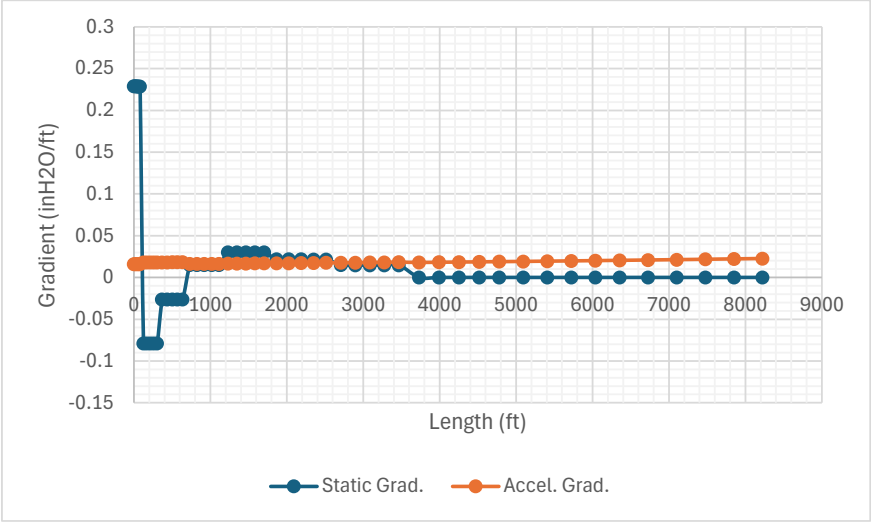

Figure 2: Pressure gradients

Furthermore, these gradients significantly affect the hydraulic performance of the pipeline and indirectly influence corrosion by controlling shear stress, water hold-up, and phase behaviour.

Static Gradient

The static gradient represents the pressure change due to elevation differences along the pipeline route. Where the pipeline rises in elevation, additional pressure is required to lift the fluid mixture, while pressure recovery occurs in downward sections.

From the simulation, the static gradient fluctuated moderately along the pipeline profile, indicating undulating terrain conditions. Such elevation changes promote liquid accumulation in low sections of the pipe, leading to water pooling. Water accumulation is dangerous because corrosion mainly occurs in areas where free water contacts the steel wall.

Friction Gradient

The friction gradient was observed to be the dominant pressure-loss mechanism throughout the pipeline length. This occurred due to wall shear stress between the flowing gas-liquid mixture and the internal pipe surface.

High friction gradients generally indicate:

i. Increased turbulence
ii. Higher wall shear stress
iii. Removal of protective scales
iv. Increased erosion-corrosion tendency

This means that regions with high friction losses are more vulnerable to localized corrosion attack.

Acceleration Gradient

The acceleration gradient was relatively small compared with static and friction gradients. This suggests that velocity changes along the pipeline were moderate and no severe compressibility effects were present.

However, in gas-condensate systems, acceleration effects can become significant where gas expansion occurs, especially near low-pressure zones.

Effect of Gradient on Corrosion

The combined effect of static and friction gradients determines where water settles and where shear stress becomes high. Therefore:

1. Low spots encourage under-deposit corrosion
2. High velocity sections encourage erosion-corrosion
3. Intermittent flow zones may worsen localized attack

Pressure Drop Profiles

Three pressure drop components were simulated:

1. Frictional pressure drop
2. Static pressure drop
3. Acceleration pressure drop

Pressure Drop due to friction

The figure 3 shows a stepwise increase in pressure drop along the pipeline length, which provides important insight into the spatial distribution of internal corrosion risk and flow-related degradation mechanisms.

At the inlet section, the relatively low but rapidly increasing pressure drop indicates the onset of strong hydrodynamic effects such as flow acceleration, phase interaction, and possible slug formation. These conditions are significant for corrosion because they increase turbulence and wall shear stress**,** which enhance the transport of corrosive species (CO_2, H_2S, water) to the pipe wall and may also initiate protective film breakdown**.** As a result, this region is typically associated with elevated risk of flow-assisted corrosion and early metal loss initiation**.**

Moving downstream, the stepwise increases in ΔP suggest repeated changes in flow resistance, likely caused by liquid holdup, phase redistribution, or developing internal roughness. Each plateau followed by a sudden rise may indicate zones where corrosion products or deposits temporarily alter flow behaviour. These deposits can create localized under-deposit corrosion cells**,** where stagnant liquid becomes trapped beneath scales, promoting pitting corrosion and localized wall thinning.

In the mid-pipeline region, the sustained increase in pressure drop reflects a progressive rise in overall flow resistance. This is often associated with internal surface roughening due to ongoing corrosion**,** scaling, or

erosion-corrosion processes. As the pipe wall deteriorates, turbulence intensity increases, which further accelerates corrosion in a feedback loop of roughness and metal loss.

At the downstream section, the higher and stabilizing ΔP values indicate a more established high-resistance flow regime. This suggests that corrosion or deposition effects have become more pronounced and stable. Such conditions are typically associated with long-term uniform corrosion combined with localized pitting, especially in wet gas systems where water continuously accumulates.

Moreover, the pressure drop profile indicates that corrosion risk is not uniform but increases in zones where step changes in ΔP occur. These zones are particularly vulnerable to:

i. Flow-assisted corrosion (high shear regions)
ii. Under-deposit and pitting corrosion (flow stagnation/plateaus)
iii. Erosion-corrosion due to turbulence and phase interaction
iv. Progressive wall thinning contributing to increased roughness

Lastly, the stepwise increase in frictional pressure drop suggests progressive deterioration of internal pipeline conditions, where corrosion, scaling, and multiphase flow effects reinforce each other. These transition zones should be prioritized for inspection, corrosion inhibition,

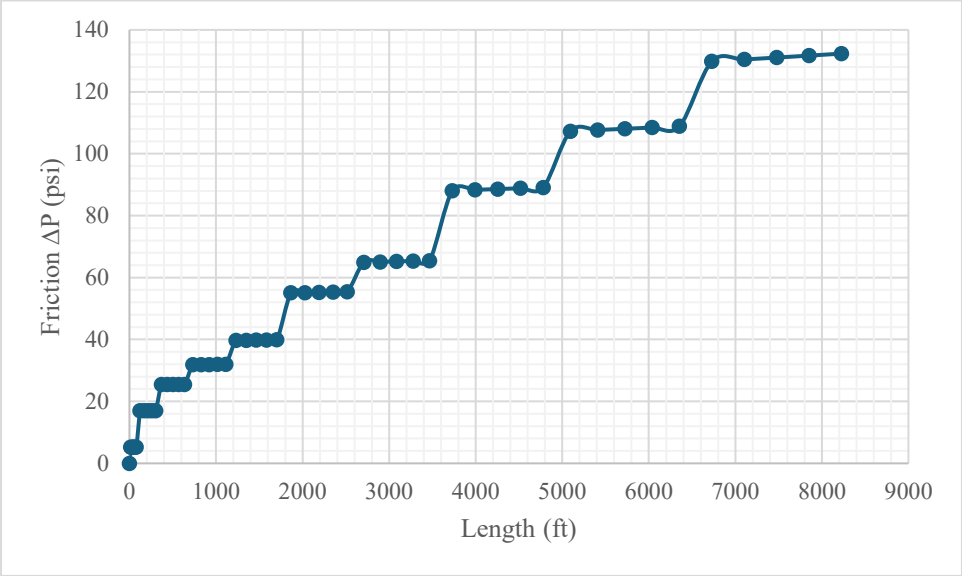

Figure 3: Frictional loss due to Pressure drop

Pressure drop due to Static and Acceleration

The figure 4 provides important insight into how hydrodynamic forces influence internal corrosion risk along the pipeline. The static pressure drop (blue line) shows strong fluctuations near the inlet (0-1000 ft), followed by stabilization and then a sharp reduction to near-zero values beyond approximately 3500 ft.

At 0-1000 ft which is highly unstable region,where the sharp negative and positive fluctuations indicate strong flow disturbances and phase interaction. This promotes:

- Local turbulence and wall shear variation
- Breakdown of protective corrosion scales
- Increased risk of erosion-corrosion and CO_2 corrosion initiation

At 1000-3500 ft which is the transition zone,

pressure drop becomes more stable, indicating improved flow regime. Corrosion risk is moderate, mainly driven by uniform CO_2 corrosion if water is present.

More so, beyond 3500 ft which is Near-zero static DP, the near-flat profile suggests very low static driving force variation, which can lead to:

- Low flow velocity zones
- Liquid holdup and stagnant pockets
- Increased likelihood of localized pitting and under-deposit corrosion

Subsequently, the acceleration pressure drop (Orange Line) increases gradually along the pipeline, indicating continuous momentum changes in the flowing mixture. This steady increase suggests persistent fluid acceleration effects and phase redistribution and supports on-going wall interaction and shear stress, which can Sustain general (uniform) corrosion, Reduce scale stability in wet gas environments and Maintain corrosive

species transport (CO_2, H_2S, water). However, the absence of abrupt spikes suggests limited risk of severe erosion-corrosion downstream.

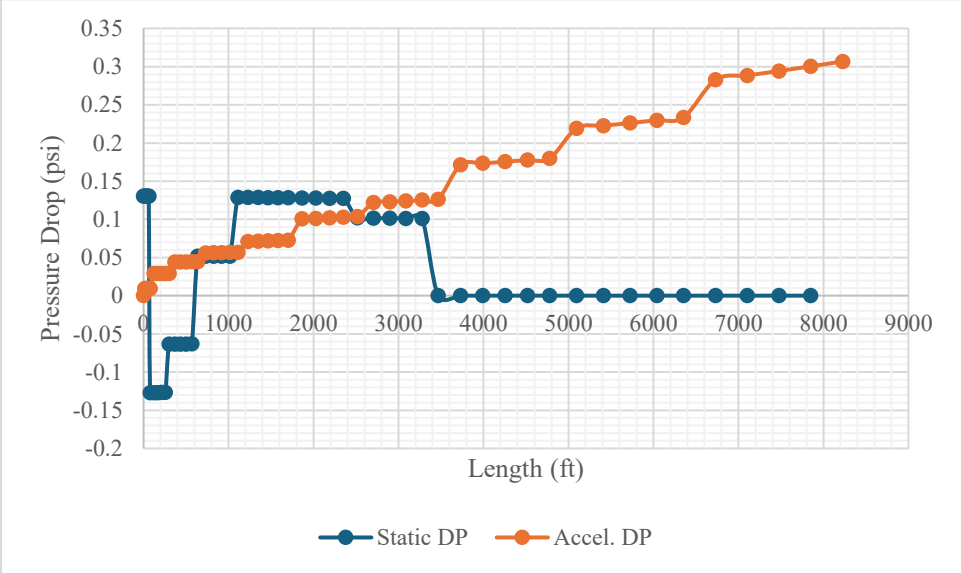

Figure 4: Pressure drop due static and acceleration

Liquid and Vapor Velocity Profiles

The figure 5 below is the liquid and vapour velocity profile in the pipeline under annular flow conditions. The vapour phase exhibits a high inlet velocity**,** which gradually decreases along the pipeline length. This reduction is primarily due to frictional pressure losses along the pipe wall, phase interaction with entrained liquid droplets and gradual expansion and energy dissipation in the gas core However, vapour typically dominates the core region and therefore carries most of the momentum, but, as pressure drops along the pipeline, vapour density slightly increases while velocity reduces, consistent with multiphase flow theory (Brill & Mukherjee, 1999). Furthermore, the liquid phase starts with **a** lower velocity at the inlet and gradually increased and stabilized downstream due to gas shear entrainment at the interface and redistribution of liquid film along the pipe wall as well as development of a more stable liquid film layer The slight fluctuations observed along the profile indicate interfacial instability and slugging tendencies, even though the dominant regime remains annular. Consequently, the high vapour velocity region corresponds to higher CO_2 corrosion rates while the liquid film regions correlate with localized corrosion and scaling behaviour and the flow development along the pipeline explains the slight reduction in corrosion rate downstream

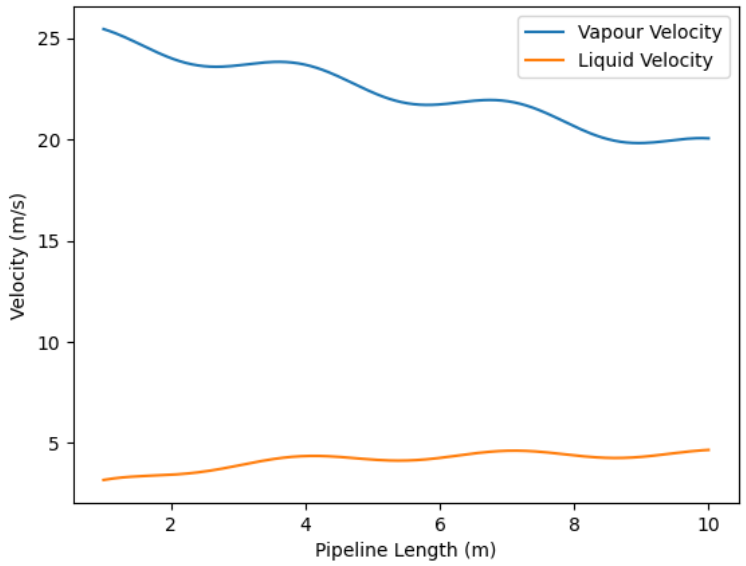

Figure 5: Liquid and Vapour velocity profile

Corrosion Rate Analysis

Two corrosion mechanisms were simulated:

1. Corrosion due to dissolved CO_2
2. Corrosion due to scale formation/removal

Corrosion rate was reported in inch per year (in/year).

The acid concentration in this study was the amount of carbonic acid formed from the mixture of water and CO_2 according to the reaction:

$$CO_2 + H_2O \leftrightarrow H_2CO_3 \qquad 5$$

As shown in the figures below for CO_2 corrosion rate and scaled corrosion rate for the different acid concentration

Effect of Pipeline Length on Corrosion Behaviour at pH 7.0

The figure 6 shows the variation of corrosion rate along the pipeline length at pH=7.0, comparing CO_2 corrosion and scaled corrosion expressed in inches per year (in/yr)**.** The CO_2 Corrosion (Blue line) is consistently higher across the pipeline whereas Scaled Corrosion (Orange line) remains significantly lower throughout the pipe length and both curves gradually decrease with increasing pipe length. The CO_2 corrosion rate starts at about 0.71 in/yr near the inlet and decreases slowly to approximately 0.66 in/yr near 8000 ft This indicated that dissolved carbon dioxide reacts with water to form carbonic acid (H_2CO_3), which aggressively attacks the steel surface and promotes internal corrosion. The high initial corrosion rate suggests severe inlet conditions caused by elevated CO_2 partial pressure, increased turbulence, and enhanced mass transfer of corrosive species to the pipe wall. The gradual decline in corrosion rate downstream may be attributed to depletion of corrosive reactants, stabilization of flow conditions, and the possible formation of a partially protective iron carbonate ($FeCO_3$) scale film on the steel surface. The scaled corrosion rate initially begins at approximately 0.14 in/yr and gradually decreases to about 0.11 in/yr along the pipeline length. This comparatively lower corrosion rate indicates the presence of protective scale deposits, such as iron carbonate ($FeCO_3$) or other mineral scales, which reduce direct metal exposure to the corrosive fluid. The deposited scale layer acts as a physical barrier between the steel surface and the surrounding environment, thereby slowing electrochemical corrosion reactions and restricting the diffusion of dissolved CO_2 to the pipe wall. Consequently, scale formation contributes significantly to corrosion mitigation by lowering the overall rate of metal loss.At neutral pH (7.0), the corrosion rate is lower than under acidic conditions due to the reduced concentration of hydrogen ions available to participate in electrochemical reactions. However, CO_2 corrosion remains significant because dissolved carbon dioxide can still react with water to form carbonic acid in wet gas systems, thereby sustaining corrosive attack on the steel surface. In addition, the formation of protective scale layers substantially enhances corrosion resistance by limiting direct contact between the metal surface and the corrosive environment, resulting in a further reduction in metal loss. The pipeline is more vulnerable to **CO_2** corrosion than scaled corrosion at pH 7.0, especially near the inlet where corrosion rate is highest. Although corrosion decreases along the pipe, the values are still significant and may require mitigation

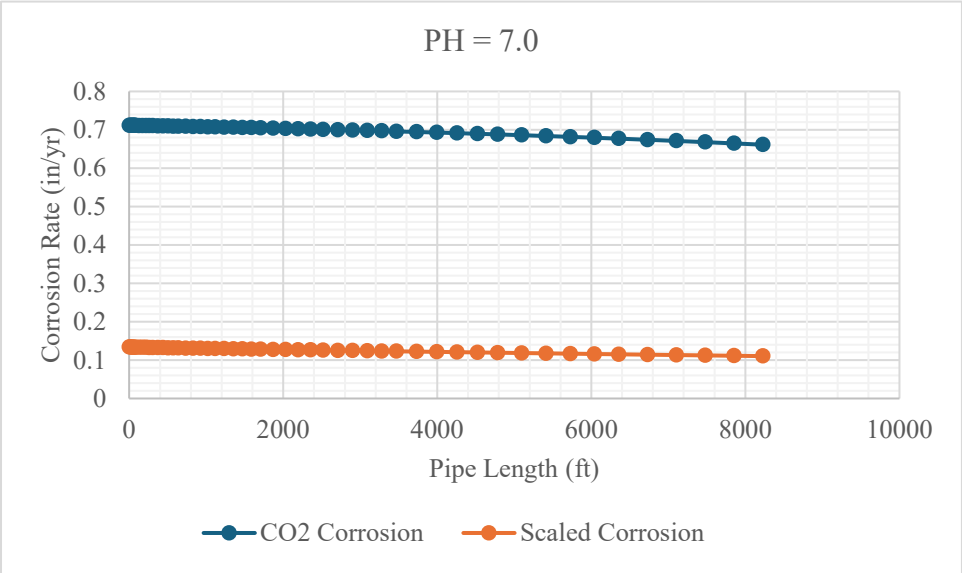

Figure 6: Corrosion Rate for pH Value of 7.0

Effect of Pipeline Length on Corrosion Behavior at pH 6.0

Figure 7 shows the predicted corrosion rates (in inches per year, in/yr) as a function of pipe length for a multiphase flow pipeline operating at a constant pH of 6.0 where two distinct corrosion mechanisms are illustrated: CO_2 corrosion (blue line) and scaled corrosion (orange line) with a simulated pipeline length of approximately 9,000 feet. The CO_2 corrosion rate was initiated near the inlet at approximately 1.08 in/yr and exhibited a gradual, almost linear decline which reached roughly 0.96 in/yr at the outlet. This represents a modest reduction of about 11% over the entire length. In contrast, the scaled corrosion rate begun significantly lower at around 0.21 in/yr and decreases more subtly to approximately 0.17 in/yr, maintaining a consistently low profile throughout the pipeline. Furthermore, the higher CO_2 corrosion rates observed are characteristic of sweet corrosion environments where dissolved carbon dioxide reacts with water to form carbonic acid, promoting anodic iron dissolution. The mild downward trend with increasing pipe length can be attributed to progressive depletion of corrodent species, changes in flow regime, or the gradual formation of protective iron carbonate ($FeCO_3$) films, which become more stable as fluid velocity or partial pressure dynamics evolve along the pipeline. The substantially lower scaled corrosion rates indicate the mitigating effect of scale formation likely iron carbonate or other mineral scales at pH 6.0. At this near-neutral pH, supersaturation with respect to $FeCO_3$ is favored, leading to precipitation that acts as a diffusion barrier, thereby suppressing the underlying electrochemical corrosion processes. The slight decline in scaled corrosion rate suggests further scale densification or thickening downstream, enhancing protectiveness.

At pH 6.0, CO_2 corrosion dominates, with rates remaining in the range of 0.95-1.08 in/yr, values that would be considered high for long-term pipeline integrity without mitigation. Scaled corrosion, however, remains below 0.22 in/yr across the entire length, demonstrating effective passivation under these conditions. The ratio of CO_2 to scaled corrosion rates varies from approximately 5:1 at the inlet to 5.6:1 at the outlet, highlighting the persistent dominance of the non-scaled mechanism. Moreso, while scale formation provides meaningful protection, it is insufficient to reduce CO_2 corrosion to acceptable levels (typically < 0.1-0.2 mm/yr or ~0.004-0.008 in/yr for carbon steel pipelines, depending on design life and safety factors). The relatively flat profiles indicate that corrosion risk is distributed along the pipeline rather than being localized at the inlet, though inlet sections experience marginally higher attack. Nevertheless, this profile underscores the importance of pH as a critical control parameter in CO_2-rich environments. Maintaining pH at or above 6.0 promotes scaling.. Overall, the figure .7 illustrates the complex interplay between corrosive species transport, scale formation kinetics, and pipeline hydrodynamics in sweet service systems.

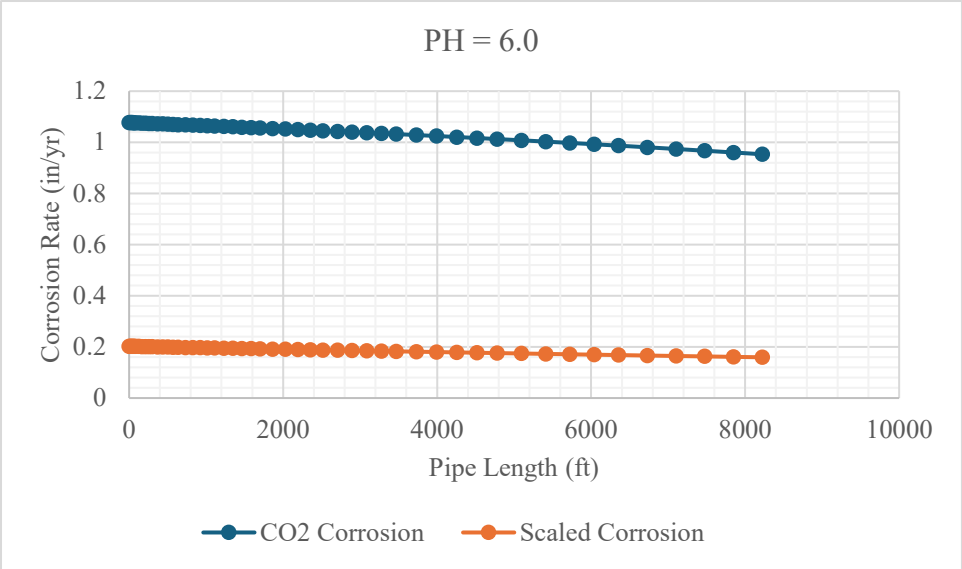

Figure 7.:Corrosion Rate Profiles Along Pipeline Length at pH 6.0

Effect of Pipeline Length on Corrosion Behavior at pH 5.0

The figure 8 illustrates the predicted corrosion rates as a function of axial pipe length for a multiphase pipeline system operating at pH 5.0 and compares two primary corrosion mechanisms: CO_2 corrosion (blue series) and scaled corrosion (orange series) over a pipeline distance of approximately 8,500 feet. The CO_2 corrosion rate commences at a high value of approximately 1.42 in/yr at the pipeline inlet and decreases gradually in a near-linear fashion to about 1.19 in/yr at the outlet. This represents a reduction of roughly 16%

over the evaluated length while the scaled corrosion rate started at approximately 0.26 in/yr and declined more discreetly to around 0.19 in/yr, remaining consistently low throughout the pipeline.

Moreso, at pH 5.0, the environment is more acidic than the previously examined pH 6.0 condition, resulting in significantly elevated overall corrosion rates. The elevated CO_2 corrosion is driven by increased dissociation of carbonic acid (H_2CO_3) and higher availability of H^+ ions, which accelerate the cathodic hydrogen evolution reaction and anodic iron dissolution. The gradual decline along the pipe length is likely attributed to progressive consumption of dissolved CO_2, increasing pH due to corrosion product formation, or the development of partially protective surface films as the fluid travels downstream. The scaled corrosion component, while higher than at pH 6.0, remains substantially lower than the CO_2 corrosion rate. This indicated that some degree of iron carbonate scaling still occurs; however, at pH 5.0 the scaling tendency is weaker due to lower supersaturation ratios, resulting in less protective or more porous scales. However, a direct comparison with the pH 6.0 case reveals the strong sensitivity of corrosion kinetics to pH. At pH 5.0, CO_2 corrosion rates are approximately 30-35% higher across the pipeline length, while scaled corrosion rates are roughly 20-25% higher. The dominance of CO_2 corrosion is more pronounced, with the ratio of CO_2 to scaled corrosion ranging from about 5.5:1 at the inlet to approximately 6.3:1 at the outlet. These results align with established corrosion models (e.g., de Waard-Milliams, NORSOK M-506, or ECE), which predict an exponential increase in corrosion rate with decreasing pH in sweet systems due to the direct relationship between pH and carbonic acid speciation. Consequently, the corrosion rates observed at pH 5.0 particularly the CO_2 corrosion values which exceeds 1.2 in/yr are critically high and would lead to rapid wall thickness loss in carbon steel pipelines. Without effective mitigation, such rates could result in pipeline failure well before design life, posing significant safety, environmental, and economic risks.. Again, the relatively uniform (yet gradually declining) corrosion profile suggests that corrosion is a distributed rather than highly localized phenomenon under these flow conditions. Nevertheless, inlet piping and fittings may still require additional attention due to higher turbulence and mass transfer effects.

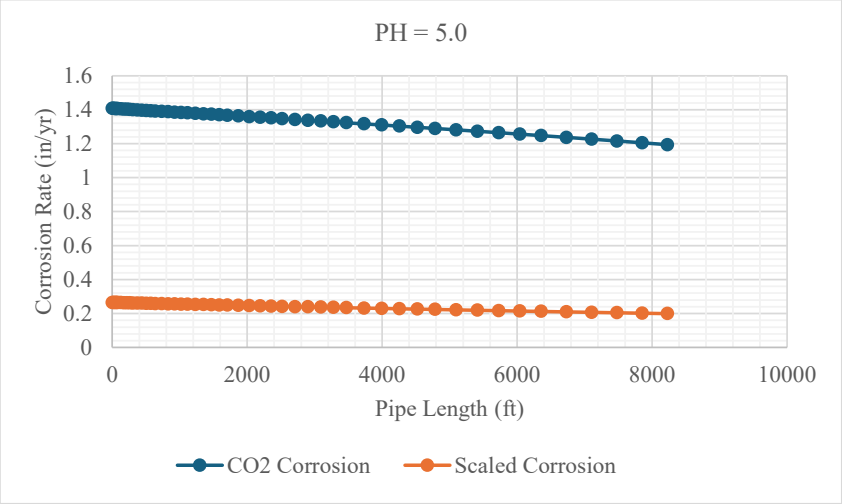

Figure 8. Corrosion Rate Profiles Along Pipeline Length at pH 5.0

Effect of Pipeline Length on Corrosion Behavior at pH 4.0

The Figure 9 shows the predicted corrosion rates (in/yr) versus pipe length for a multiphase pipeline operating at pH 4.0. Unlike the previous cases (pH 5.0 and 6.0), the legend is reversed: the CO_2 corrosion rate is represented by the orange line, while the scaled corrosion rate is shown by the blue line. The simulation covers approximately 8,500 feet of pipeline length. The CO_2 corrosion rate started at a very high value of approximately 1.65 in/yr at the inlet and decreased gradually to about 1.36 in/yr at the outlet, representing a reduction of roughly 17% along the pipeline. In contrast, the scaled corrosion rate began much lower at approximately 0.32 in/yr and declined steadily to around 0.22 in/yr by the end of the section. Furthermore, at pH 4.0, the system is significantly more acidic, leading to a sharp increase in CO_2 corrosion kinetics. The lower pH shifted the carbonic acid equilibrium, substantially increasing the concentration of H^+ and undissociated H_2CO_3, which strongly accelerated both cathodic and anodic reactions. This resulted in CO_2 corrosion rates that are markedly higher than those observed at pH 5.0 and pH 6.0. The scaled corrosion rates remained relatively suppressed, indicating that while some scale formation (primarily $FeCO_3$) still occurs, its protectiveness is limited under these highly acidic conditions. The gradual decline in both rates along the pipe length is consistent with progressive corrodent depletion, increasing iron ion concentration, and partial surface film development as

the fluid flows downstream. However, the protective capability of the scale is clearly insufficient to counteract the aggressive acidic environment.Moreso, the data revealed a strong inverse relationship between pH and CO_2 corrosion rate. As pH decreases from 7.0 -4.0, the dominant CO_2 corrosion rate increases dramatically:
pH 7.0: ~0.71 → 0.66 in/yr
pH 6.0: ~1.08 → 0.96 in/yr
pH 5.0: ~1.42 → 1.19 in/yr
pH 4.0: ~1.65 → 1.36 in/yr

At pH 4.0, CO_2 corrosion was overwhelmingly dominant, with rates 5 to 6 times higher than the corresponding scaled corrosion throughout the pipeline. This highlights the critical threshold behaviour of iron carbonate scaling: scaling becomes far less effective below pH 5.0-5.5 in typical sweet corrosion systems. Consequently, the corrosion rates predicted at pH 4.0 are extremely severe. CO_2 corrosion rates exceeding 1.3 in/yr would cause rapid metal loss in conventional carbon steel pipelines, likely resulting in premature failure, leaks, or ruptures within months rather than years. Such conditions demand immediate and robust mitigation measures From a design standpoint, operating at pH 4.0 should be avoided wherever possible through upstream process optimization (e.g., better separation, dehydration, or pH adjustment). The distributed nature of the corrosion profile (highest at the inlet) suggests that inlet piping, manifolds, and flowlines are at greatest risk. This figure .9 reinforces the extreme sensitivity of CO_2 corrosion to pH and emphasizes the need for integrated corrosion management strategies early in the project lifecycle

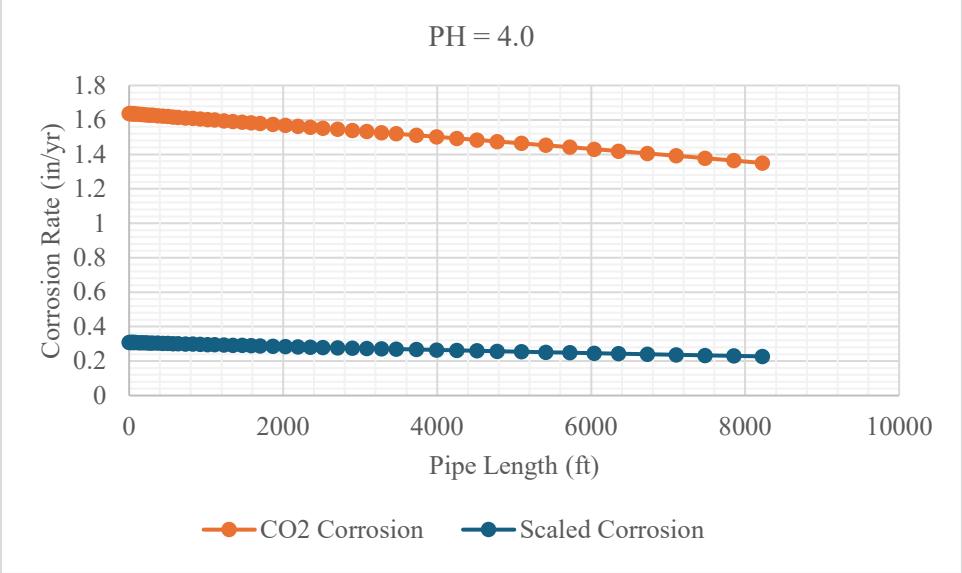

Figure 9:. Corrosion Rate Profiles Along Pipeline Length at pH 4.0

Flow Velocity Analysis and Erosion Risk Assessment

Figure 10 presents the variation of fluid velocity (orange line) and erosion velocity (green line) as a function of pipeline length. The analysis covered approximately 8,500 feet of pipeline under steady-state multiphase flow conditions. The fluid velocity started at approximately 66 ft/sec near the inlet and exhibited a gradual, almost linear increase, which reached about 72 ft/sec at the outlet. In contrast, the erosion velocity remained nearly constant at approximately 20 ft/sec throughout the entire pipeline length. Furthermore, the observed increase in fluid velocity along the pipeline is typical in multiphase gas-dominated or wet gas systems. As pressure drops due to frictional losses and elevation changes, the gas expands, leading to higher volumetric flow rates and consequently increased mixture velocity. This acceleration effect is more pronounced in long pipelines with significant pressure decline. The erosion velocity (also referred to as erosional velocity limit) is calculated based on industry standards such as API RP 14E, which typically uses the equation 3.3. The near-constant erosion velocity in figure 4.10 suggests relatively stable fluid density or consistent application of the erosional velocity criterion along the pipeline. Consequently, a critical finding from figure 4.10 is the substantial margin between actual fluid velocity and the erosional velocity limit. Throughout the pipeline fluid velocity ranges from 66 to 72 ft/sec and erosion velocity remains stable at ≈20 ft/sec**.** This resulted in the fluid velocity consistently exceeding the erosional velocity limit by a factor of 3.3 to 3.6**.** According to API RP 14E guidelines, exceeding the erosional velocity limit indicates a high potential for erosional damage, particularly in systems containing sand, solids, or high-velocity liquid droplets that can cause mechanical wear on pipe walls, elbows, tees, and fittings. The risk is further amplified at higher velocities toward the outlet of the pipeline,

where the greatest velocity was observed. In multiphase flow, erosion-corrosion synergy may also occur, where high shear stresses strip away protective scales or inhibitor films, exposing the metal to accelerated CO_2 corrosion (as observed in previous pH sensitivity analyses). However, the results presented in Figure 4.10 revealed severe erosion risk across the entire pipeline length. Operating at fluid velocities more than three times the calculated erosional limit is generally unacceptable for long-term integrity and could lead to rapid wall thinning, especially in carbon steel systems..Again, when viewed alongside the pH-dependent corrosion rate profiles (Figures X.Y at pH 7.0, pH 6.0, 5.0, and 4.0), the high fluid velocities identified here suggest a strong erosion-corrosion interaction. High shear forces can prevent stable scale formation, explaining the relatively limited effectiveness of scaled corrosion mechanisms observed in earlier analyses. This synergy could result in corrosion rates significantly higher than those predicted by pure CO_2 corrosion models. This velocity analysis underscores the necessity of integrated flow assurance and corrosion management studies during the conceptual and FEED (Front End Engineering Design) stages of pipeline projects.

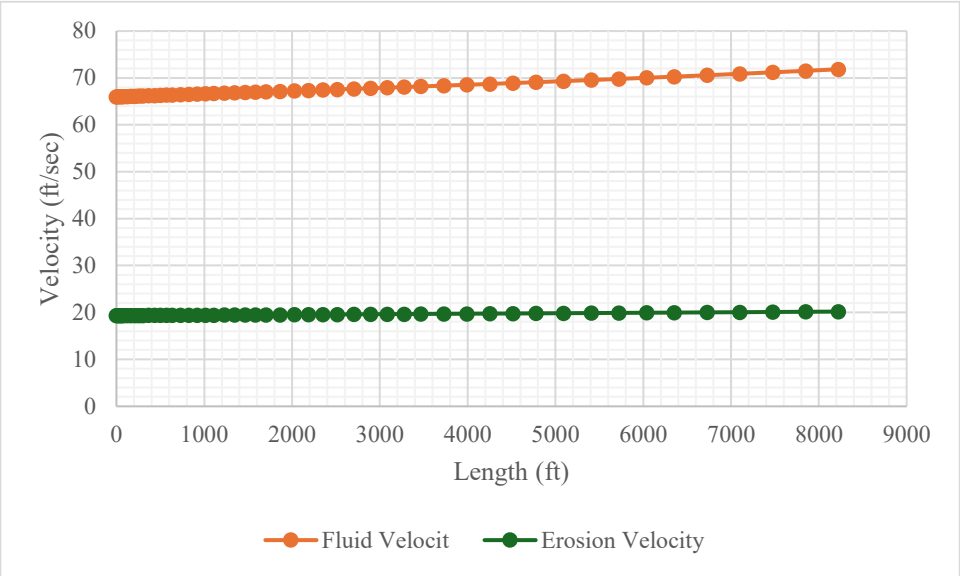

Figure 10: Fluid Velocity and Erosion Velocity Profiles Along Pipeline Length

Conceptual Corrosion Mitigation Method: Integrated pH-Velocity-Corrosion Management Strategy (PVCMS)

This study proposes a Conceptual Integrated pH-Velocity-Corrosion Management Strategy (PVCMS) designed specifically for wet gas pipelines operating under similar conditions. The PVCMS is a multi-layered approach that simultaneously addresses the three primary drivers of corrosion identified in this simulation: low pH**,** excessive velocity/erosion**,** and inadequate scaling**.**

Key Components of PVCMS

Phase 1: Upstream pH Stabilization

1. Continuous injection of alkaline chemicals at the wellhead or manifold to maintain bulk fluid pH between 6.0 and 6.5.
2. Expected benefit: Reduction of CO_2 corrosion rate by 40-60% and enhancement of protective $FeCO_3$ scale formation.

Phase 2: Flow Velocity Optimization

1. Installation of a larger-diameter (12-14 inch) spool or flow diffuser at the inlet section (first 1,000-2,000 ft) to reduce inlet velocity.
2. Strategic placement of velocity control orifices or choke valves to maintain mixture velocity below 30-35 ft/sec (well within API RP 14E limits).

Phase 3: Chemical and Mechanical Mitigation

1. High-dose corrosion inhibitor injection (tailored for high-shear, sweet service).
2. Periodic batch inhibition and pigging program (foam pigs followed by inhibitor slugs) to clean deposits and renew protective films.
3. Use of drag-reducing agents (DRA) where applicable to lower frictional pressure losses.

Phase 4: Material and Design Enhancements

1. Application of internal epoxy coating or glass-reinforced plastic (GRP) lining in high-risk zones.

2. Use of erosion-resistant elbows and fittings (e.g., long-radius, hardened, or clad).

Phase 5: Real-Time Monitoring and Feedback

1. Deployment of a Supervisory Control and Data Acquisition (SCADA) integrated corrosion monitoring system with wireless sensors.
2. Development of a risk-based inspection (RBI) plan with dynamic adjustment based on real-time pH, velocity, and corrosion rate data.

Expected Performance

Implementation of the full PVCMS is projected to reduce overall corrosion rates to below 0.05 in/yr (acceptable industry threshold for carbon steel) while maintaining pipeline integrity over a 25–30 year design life.

IV. CONCLUSION

This study investigated the internal corrosion behaviour of a 10-inch wet gas pipeline through multiphase flow simulation using Aspen HYSYS**,** , with particular emphasis on the influence of flow dynamics, pressure gradients, fluid velocities, erosion tendencies, and pH (acid concentration) on CO_2 corrosion and scaled corrosion rates.The simulation results revealed that CO_2 corrosion is the dominant degradation mechanism across all tested pH levels (4.0-7.0), with rates ranging from 0.66 in/yr at pH 7.0 to as high as 1.65 in/yr at pH 4.0. Although protective iron carbonate scale formation provided some mitigation, its effectiveness diminished significantly under more acidic conditions. Corrosion rates were consistently highest at the pipeline inlet due to elevated turbulence, higher partial pressure of CO_2, and enhanced mass transfer, and decreased gradually downstream.

A critical finding of this study is the severe erosion risk identified in the velocity analysis. Actual fluid velocities (66-72 ft/sec) exceeded the API RP 14E erosional velocity limit (≈20 ft/sec) by a factor of 3.3-3.6 throughout the pipeline length. This condition created a strong erosion-corrosion synergy, whereby high wall shear stress removes protective scales and inhibitor films, thereby accelerating metal loss beyond what pure CO_2 corrosion models predict. Gradient and pressure drop profiles further demonstrated that corrosion risk is not uniform along the pipeline. High-risk zones were identified at the inlet (0-800 ft) due to flow instability and turbulence, and in low-velocity sections where liquid hold-up and under-deposit corrosion are likely. Friction gradient was the dominant pressure loss mechanism, directly influencing wall shear stress and flow-assisted corrosion. Overall, the results confirmed that without effective intervention, the studied pipeline faces a high probability of premature failure, particularly under low pH and high-velocity conditions. The findings underscore the complex interplay between multiphase hydrodynamics, pH, scaling tendency, and erosion in sweet gas service environments.

Reference

[1]. Gurbanov, S. (2021). Role of Natural Gas Consumption in the Reduction of CO_2 Emissions: Evidence from Azerbaijan. Energies, 14(22), 7695. https://doi.org/10.3390/en14227695

[2]. Joseph, O. O., Banjo, S., Babaremu, K., & Ogunlana, O. (2022). Global and economic effects of corrosion - An overview. AIP Conference Proceedings, 2437(1), Article 020149. https://doi.org/10.1063/5.0092286

[3]. Koch, G. H., Varney, J., Thompson, N., Moghissi, O., Gould, M., & Payer, J. (2016). International Measures of Prevention, Application, and Economics of Corrosion Technologies (IMPACT) Study. NACE International (now AMPP). Houston, TX. Report No. OAPUS310GKOCH (AP110272).: http://impact.nace.org

[4]. Bu, F., Lu, Q., Jia, B., Gao, X., Zhang, H., Wang, W., & Wang, Z. (2025). A review of research on leakage and diffusion characteristics of buried gas pipelines. Journal of Pipeline Science and Engineering, 100426. https://doi.org/10.1016/j.jpse.2025.100426

[5]. Rusin, A., & Stolecka, K. (2021). Analysis of the effects of failure of a gas pipeline caused by a mechanical damage. Energies, 14(22), 7686. https://doi.org/10.3390/en14227686

[6]. Liu, Y., Zhang, H., Wang, J., & Chen, X. (2025). Hybrid machine learning models for corrosion rate prediction in natural gas pipelines. *Applied Sciences, 15*(4),15-23.

[7]. Lu, H., Cheng, F., & Shan, Y. (2023). An inventory of greenhouse gas emissions due to natural gas pipeline incidents in the United States and Canada from the 1980s to 2021. Scientific Data, 10, Article 359. https://doi.org/10.1038/s41597-023-02177-0

[8]. Askari, M., Aliofkhazraei, M., & Afroukhteh, S. (2019). A comprehensive review on internal corrosion and cracking of oil and gas pipelines. Journal of Natural Gas Science and Engineering, 71, 102971. https://doi.org/10.1016/j.jngse.2019.10297

[9]. Nešić, S. (2007). Key issues related to modelling of internal corrosion of oil and gas pipelines – A review. *Corrosion Science, 49*(12), 4308–4338. https://doi.org/10.1016/j.corsci.2007.06.006

[10]. Revie, R. W., & Uhlig, H. H. (2025). Corrosion and corrosion control: An introduction to corrosion science and engineering (5th ed.). Wiley. https://doi.org/10.1002/9781119324751

[11]. Brill, J. P., & Mukherjee, H. (1999). Multiphase Flow in Wells. SPE Monograph Series, Volume 17. Richardson, Texas: Society of Petroleum Engineers.